Optical Properties of Overfire Soot in Buoyant Turbulent Diffusion Flames at Long Residence Times

Ü. Ö. Köylü
Research Fellow.

G. M. Faeth
Professor.
Fellow ASME

Department of Aerospace Engineering,
The University of Michigan,
Ann Arbor, MI 48109-2140

The optical properties of soot were studied for the fuel-lean (overfire) region of buoyant turbulent diffusion flames in still air. Results were limited to the long residence time regime where soot structure is independent of position in the overfire region and residence time for a particular fuel. Measurements included scattering, absorption, and extinction cross sections at 514.5 nm and extinction cross sections at 632.8 and 1152 nm for flames fueled with acetylene, propylene, ethylene, and propane. The measurements were used to evaluate scattering predictions based on the Rayleigh-Debye-Gans (RDG) approximation for randomly oriented polydisperse fractal aggregates of spherical primary soot particles having constant diameters. The present soot aggregates exhibited significant departures from Rayleigh-scattering behavior at 514.5 nm, with forward scattering roughly 100 times larger than wide-angle scattering and ratios of scattering to absorption cross sections in the range 0.22–0.41, increasing with increasing propensity of the fuel to soot. The approximate RDG theory generally provided an acceptable basis to treat the optical properties of the present overfire soot aggregates, although additional measurements in the Guinier (small angle) regime are needed for a definitive evaluation of model performance.

Introduction

Soot optical properties must be understood in order to estimate continuum radiation from flames and to develop nonintrusive laser-based methods for measuring soot properties. Estimating soot optical properties is challenging, however, because soot structure is complex. In particular, although soot consists of small spherical primary particles that generally satisfy the Rayleigh scattering approximation, the primary particles collect into wispy aggregates that do not exhibit either simple Rayleigh or Mie scattering behavior (Erickson et al., 1964; Dalzell et al., 1970; Wersborg et al., 1973; Magnussen, 1974). In spite of the complexities, however, potentially effective theories of soot optical properties have been developed based on mass fractal concepts; see Jullien and Botet (1987), Martin and Hurd (1987), Dobbins and Megaridis (1991), and references cited therein. Nevertheless, these methods have not been directly evaluated at conditions where both soot structure and optical properties are known (Köylü and Faeth, 1993). Thus, the objective of the present investigation was to undertake such an evaluation by completing measurements of soot optical properties at conditions where Köylü and Faeth (1992) had recently completed measurements of soot structure. In addition, the existing theories were extended in order to resolve problems disclosed by the present evaluation.

The soot structure measurements of Köylü and Faeth (1992) were carried out in the fuel-lean (overfire) region of buoyant turbulent diffusion flames burning in still air within the long residence time regime, where characteristic flame residence times are roughly an order of magnitude longer than the laminar smoke point residence time. These conditions are of interest because overfire soot aggregates are large, providing a stringent test of theories of soot optical properties. Additionally, soot structure for a particular fuel in the long residence time regime is independent of position in the overfire region and residence time, which both simplifies measurements of optical properties and provides results of some general interest for studies of flame radiation. The structure measurements were carried out by thermophoretic sampling and analysis using transmission electron microscopy (TEM). The findings include fractal dimensions, and the probability density distributions of primary particle diameters and the number of primary particles in aggregates, for a variety of gaseous and liquid fuels. Present measurements included scattering, absorption, and extinction cross sections at 514.5 nm, and extinction cross sections at 632.8 and 1152 nm, for flames fueled with acetylene, propylene, ethylene, and propane.

The paper begins with descriptions of experimental and theoretical methods. This is followed by results, considering estimates of soot structure parameters from scattering measurements, angular scattering patterns, and extinction properties, in turn. The present discussion is brief, additional details, and a complete tabulation of data can be found in Köylü (1992).

Experimental Methods

Apparatus. A sketch of the test apparatus appears in Fig. 1. The arrangement was the same as for the soot structure measurements of Köylü and Faeth (1992) except for the presence of a soot collection system needed for the scattering measurements. Combustion was in still air with the burners located within a large enclosure (2.4 × 2.4 × 3.6 m high). The enclosure had a metal hood at the top and an adjustable exhaust system to collect and remove combustion products. The side walls of the enclosure were plastic strips to minimize effects of room disturbances. A water-cooled burner having an exit diameter of 50 mm, described by Sivathanu and Faeth (1990), was used to yield strongly buoyant, pool-like turbulent flames in the long residence time regime.

Soot optical properties were measured by collecting the combustion products in a heated sampling duct (to prevent thermophoretic deposition of soot on the duct surfaces). The duct had a 152-mm-dia exhaust at the top, which discharged into the main hood of the apparatus. Measurements showed that mixing within the heated duct was sufficient to yield uniform soot and gas species concentrations across the exit of the exhaust duct where the scattering and extinction measurements

Contributed by the Heat Transfer Division for publication in the JOURNAL OF HEAT TRANSFER. Manuscript received by the Heat Transfer Division August 1992; revision received May 1993. Keywords: Fire/Flames, Radiation, Radiation Interactions. Associate Technical Editor: W. L. Grosshandler.

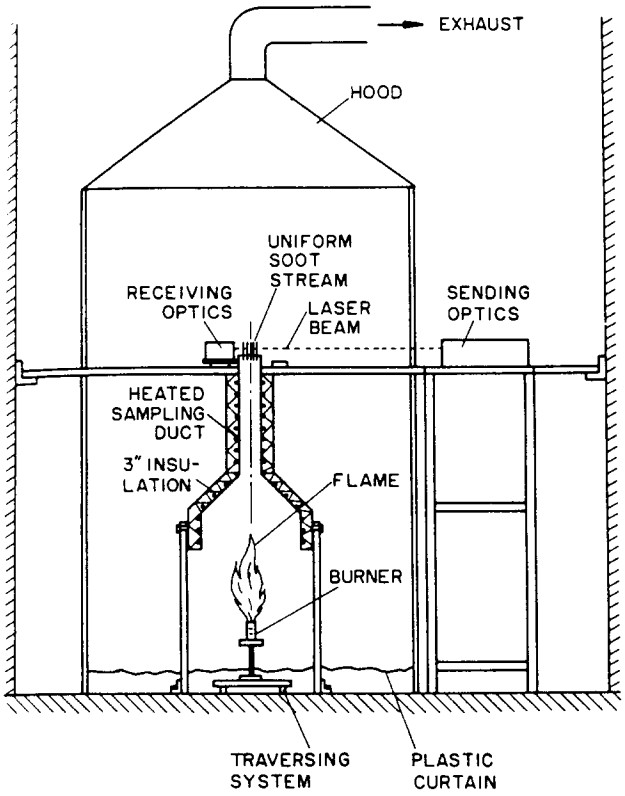

Fig. 1 Sketch of the experimental apparatus

were made. Note that since soot structure is independent of position in the overfire region at long residence time conditions, collection in this manner does not affect soot structure properties.

Scattering Measurements. An argon-ion laser having an optical power of 1.7 W at 514.5 nm was used for the scattering measurements. The incident laser beam was passed through a polarization rotator and a mechanical chopper (operating at 1250 Hz) before being focused at the center of the exhaust duct using a 1000 mm focal length lens. This yielded a waist diameter of 260 μm and a confocal length of roughly 400 mm. The collecting optics were mounted on a turntable surrounding the exhaust duct so that scattering angles, θ = 5–160 deg, could be considered. The collecting optics consisted of an 85 mm focal length lens, a dichroic sheet polarizer, a laser line filter (1 nm bandwidth), and a photomultiplier. The lens aperture defined a solid collection angle of 0.7 msr with a 1 mm long sampling volume at θ = 90 deg, which increased to roughly 11 mm at θ = 5 deg. Neutral-density filters were used in the optical path to control the dynamic range of detection. The experimental area as well as the receiving optics were covered with black cloth to reduce optical noise from the room lighting and the flame. The detector output passed through a lock-in amplifier and was stored on a computer, sampling at 500 Hz for 10 s and averaging five sampling intervals to achieve a repeatability within 10 percent.

The angular light scattering system was calibrated by measuring Rayleigh scattering from nitrogen gas. After correction for the reciprocal sin θ dependence of the scattering volume, the *vv* and *hh* differential cross sections were within 10 percent of Rayleigh scattering predictions for θ = 5–160 deg. Absolute volumetric differential scattering cross sections of soot were found from ratios of the detector signal for soot and nitrogen, after accounting for signal attenuation in the optical path for soot, based on the nitrogen optical properties of Rudder and Bach (1968). Total volumetric scattering cross sections were found by integrating the volumetric differential scattering cross sections over the whole spherical surface. This required extrapolation of the measurements to reach θ = 0 and 180 deg; however, uncertainties caused by the extrapolations were small due to the relatively small solid angle involved for forward scattering and the relatively slow variation of scattering with θ in the backward direction. The overall experimental uncertainties (95 percent confidence) of the angular and the total light scattering measurements were comparable and were estimated to be less than 20 percent, dominated by finite sampling

Nomenclature

C = optical cross section
d_p = primary particle diameter
D_f = mass fractal dimension
$E(m)$ = refractive index function = $Im((m^2 - 1)/(m^2 + 2))$
$f(q\ R_g)$ = aggregate form factor, Eq. (3)
f_{VA}, f_{VR} = soot volume fractions from aggregate and Rayleigh theories
$F(m)$ = refractive index function = $|(m^2 - 1)/(m^2 + 2)|^2$
$g(kR_g, D_f)$ = aggregate total scattering factor, Eq. (7)
i = $(-1)^{1/2}$
k = wave number = $2\pi/\lambda$
k_f = fractal prefactor, Eq. (1)
m = refractive index of soot = $n + i\kappa$
n = real part of refractive index of soot
n_a = mean number of aggregates per unit volume
n_p = mean number of primary particles per unit volume
N = number of primary particles per aggregate
N_c = aggregate size for onset of power-law regime, Eq. (16)
N_g = geometric mean number of primary particles per aggregate
$p(N)$ = probability density function of aggregate size
q = modulus of scattering vector = $2k \sin(\theta/2)$
Q = volumetric optical cross section
R_g = radius of gyration of an aggregate
x_p = primary particle size parameter = $\pi d_p/\lambda$
β = aggregate scattering parameter = $3D_f/(8k^2R_g^2)$
θ = angle of scattering from forward direction
κ = imaginary part of refractive index of soot
λ = wavelength of radiation
ρ_{sa} = ratio of scattering to absorption cross section
ρ_v = depolarization ratio
σ_g = geometric standard deviation of aggregate size distribution

Subscripts

a = absorption
d = differential
e = extinction
h = horizontal polarization
ij = incident (i) and scattered (j) polarization direction
s = total scattering
v = vertical polarization

Superscripts

a = aggregate property
p = primary particle property
$\bar{(\ )}$ = mean value over a polydisperse aggregate population

times, the finite aperture of the detector, and the angular uncertainty of the collecting optics.

Extinction Measurements. Volumetric extinction cross sections were measured at 514.5 nm using the argon-ion leaser, and at 632.8 and 1152 nm using 15 and 40 mW HeNe lasers, respectively. Laser power meters were used to measure the intensity of the beams before and after crossing the 152-mm-long path through the exhaust flow. The extinction ratio was found by sampling at 500 Hz for 20 s and averaging five sampling intervals to achieve a repeatability within 5 percent. Experimental uncertainties (95 percent confidence) of these measurements were generally less than 20 percent, largely controlled by the magnitude of the extinction ratio and finite sampling times. Volumetric absorption cross sections were found by subtracting the total scattering cross sections from the extinction cross sections, yielding uncertainties (95 percent confidence) generally less than 20 percent.

Theoretical Methods

General Description. Predictions of soot optical properties were based on methods described by Jullien and Botet (1987), Martin and Hurd (1987), and Dobbins and Megaridis (1991). These methods were extended, however, to improve the treatment of polydisperse aggregate populations in view of the large size and broad size distributions of the present overfire soot. Major assumptions with respect to aggregate structure are as follows: spherical primary particles having constant diameters, primary particles just touching one another, uniform refractive indices, log-normal aggregate size distributions, and the aggregates are mass fractal-like objects. The mass fractal approximation implies the following relationship between the number of particles in an aggregate and its radius of gyration (Jullien and Botet, 1987):

$$N = k_f (R_g/d_p)^{Df} \tag{1}$$

The assumptions of nearly constant diameter spherical primary particles, log-normal size distributions, and mass fractal-like behavior are justified by the soot structure measurements for present conditions (Köylü and Faeth, 1992). The remaining assumptions are typical of past treatments of soot optical properties; see Köylü and Faeth (1993) and references cited therein.

Scattering was found using the Raleigh-Debye-Gans (RDG) approximation where effects of multiple- and self-scattering are ignored so that the electric field of each primary particle is the same as the incident electric field, and differences of the phase shift of scattered light from various points within a particular primary particle are ignored. RDG scattering requires that both $|m-1| \ll 1$ and $2x_p|m-1| \ll 1$ (Kerker, 1969; van de Hulst, 1957; Bohren and Huffman, 1983), which is questionable for soot aggregates due to the relatively large refractive indices of soot. In addition, recent computational studies suggest significant effects of multiple scattering for aggregates typical of overfire soot; see Berry and Percival (1986), Chen et al. (1990), Ku and Shim (1992), and Nelson (1989). Thus, use of RDG theory can only be justified by its capabilities to treat measured soot optical properties effectively, which was the main motivation for the present investigation.

Single Aggregates. Under the present approximations, individual primary particles satisfy the Rayleigh scattering approximation, yielding the following expressions for their optical properties (Bohren and Hoffman, 1983; Kerker, 1969):

$$C_a^p = 4\pi x_p^3 E(m)/k^2,\ C_s^p = 8\pi x_p^6 F(m)/(3k^2),\ C_{vv}^p = x_p^6 F(m)/k^2 \tag{2}$$

where $C_{hv}^p = C_{vh}^p \approx 0$, $C_{hh}^p = C_{vv}^p \cos^2\theta$ and $C_e^p = C_a^p + C_s^p$. The cross sections in Eq. (2) will be used in the following to normalize aggregate optical cross sections. The treatment of aggregate optical properties will begin with the scattering cross sections found for fractal aggregates under the RDG approximation (Kerker, 1969):

$$C_{vv}^a(\theta) = C_{hh}^a(\theta)/\cos^2\theta = N^2 C_{vv}^p f(qR_g) \tag{3}$$

where the form factor, $f(qR_g)$, is expressed as follows in the Guinier (small-angle) and power law (large-angle) regimes, respectively (Jullien and Botet, 1987; Martin and Hurd, 1987; Dobbins and Megaridis, 1991):

$$f(qR_g) = \exp(-(qR_g)^2/3), \quad \text{Guinier regime} \tag{4}$$

$$f(qR_g) = (qR_g)^{-D_f}, \quad \text{power-law regime} \tag{5}$$

where the boundary between the Guinier and power-law regimes is taken to be $(qR_g)^2 = 3D_f/2$, following Dobbins and Megaridis (1991). Within the present approximations, $C_{hv}^a = C_{vh}^a = 0$ so that the differential scattering cross section for unpolarized light becomes:

$$C_d^a(\theta) = (C_{vv}^a(\theta) + C_{hh}^a(\theta))/2 = C_{vv}^a(\theta)(1+\cos^2\theta)/2 \tag{6}$$

The total scattering cross section can be found by integrating Eq. (6) over the whole spherical surface to yield:

$$C_s^a = N^2 C_s^p g(kR_g, D_f) \tag{7}$$

The aggregate total scattering factor, $g(kR_g, D_f)$, takes on different forms depending on whether the power-law regime is reached for $\theta \le 180$ deg, as follows:

$$g(kR_g, D_f) = 1 - 2(kR_g)^2/3,\ (kR_g)^2 \le 3D_f/8 \tag{8}$$

$$g(kR_g, D_f) = \frac{\beta}{2}(3 - 3\beta + 2\beta^2) - \frac{(kR_g\beta)^2}{3} \times (3 - 4\beta + 3\beta^2) + (2kR_g)^{-D_f} \left[\frac{3}{2-D_f} - \frac{12}{(6-D_f)(4-D_f)} - 3\beta^{1-D_f/2} \times \left(\frac{1}{2-D_f} - \frac{2\beta}{4-D_f} + \frac{2\beta^2}{6-D_f}\right)\right],\ (kR_g)^2 > 3D_f/8 \tag{9}$$

At this point, the present treatment departs from Dobbins and Megaridis (1991) for single aggregates, which was limited to the Guinier regime, i.e., Eq. (8).

Based on the simulations of Nelson (1989) and Chen et al. (1990), it is assumed that absorption is not affected by aggregation, yielding

$$C_a^a = N\, C_a^p \tag{10}$$

The extinction cross section is the sum of the absorption and scattering cross sections, i.e.,

$$C_e^a = C_a^a + C_s^a = NC_a^p(1 + \rho_{sa}^a) \tag{11}$$

where

$$\rho_{sa}^a = \rho_{sa}^p\, Ng(kR_g, D_f) \tag{12}$$

The parameters ρ_{sa}^p and ρ_{sa}^a are the ratio of scattering to absorption cross sections for primary particles and aggregates, respectively. For aggregates, ρ_{sa}^a represents the error in soot volume fraction determinations when extinction measurements are processed using the Rayleigh scattering approximation (which implies $\rho_{sa}^a \approx 0$). At the limit of large aggregates, ρ_{sa}^a saturates to a value that is independent of N, where Eqs. (9) and (12) yield:

$$\rho_{sa}^a = \rho_{sa}^p k_f (4x_p)^{-D_f}(3/(2-D_f) - 12/((6-D_f)(4-D_f))) \tag{13}$$

This behavior is fundamentally different from Mie scattering for an equivalent spherical aggregate, where ρ_{sa}^a continues to increase as N increases, as discussed by Berry and Percival (1986), Nelson (1989), and Dobbins and Megaridis (1991).

Polydisperse Aggregate Populations. The mean optical cross sections of populations of randomly oriented polydis-

perse aggregates (polydisperse aggregates) are found by integrating over all aggregate sizes, as follows:

$$\overline{C}_j^a = \int_{N=1}^{\infty} C_j^a(N) p(N) dN; \quad j = pp, s, a \tag{14}$$

where $p(N)$ is the log-normal size distribution function from Köylü and Faeth (1992). Continuing the assumption that $C_{hv}^a = C_{vh}^a \approx 0$, the expression for the differential scattering cross sections of polydisperse aggregates becomes

$$\overline{C}_{vv}^a(\theta)/C_{vv}^p = \overline{C}_{hh}^a(\theta)/(C_{vv}^p \cos^2\theta)$$

$$= \int_{N=1}^{N_c} N^2 \exp(-q^2 R_g^2/3) p(N) dN + \int_{N=N_c}^{\infty} N^2 (qR_g)^{-D_f} p(N) dN \tag{15}$$

where

$$N_c = k_f (3D_f/(2q^2 d_p^2))^{D_f/2} \tag{16}$$

is the aggregate size at the matching point between the Guinier and power-law regimes, and differs for each angle. Equation (15) must be integrated numerically for general variations of aggregate size and scattering angle; however, simple limits are obtained for the Guinier and large-angle regimes. In the Guinier regime, $p(N) \ll 1$ for $N \geq N_c$ and the contribution of the second integral in Eq. (15) is negligible, yielding (Guinier and Fournet, 1955):

$$\overline{C}_{vv}^a(\theta)/(\overline{N}^2 C_{vv}^p) = 1 - q^2 \overline{R}_g^2/3 + \ldots \approx \exp(-q^2 \overline{R}_g^2/3), \quad \text{Guinier regime} \tag{17}$$

where

$$\overline{R}_g^2 = \int_{N=1}^{\infty} [R_g(N)]^2 N^2 p(N) dN / \int_{N=1}^{\infty} N^2 p(N) dN, \quad \text{Guinier regime} \tag{18}$$

In the power-law regime, $p(N) \ll 1$ for $N \leq N_c$ and the contribution of the first integral in Eq. (15) is negligible, yielding (Köylü, 1992):

$$\overline{C}_{vv}^a(\theta) / C_{vv}^p = \overline{N} k_f (qd_p)^{-D_f} = \overline{N}^2 (q^2 \overline{R}_g^2)^{-D_f/2}, \quad \text{power-law regime} \tag{19}$$

where

$$\overline{R}_g^2 = \left[\int_{N=1}^{\infty} [R_g(N)]^{2D_f} p(N) dN / \int_{N=1}^{\infty} [R_g(N)]^{D_f} p(N) dN \right]^{2/D_f}, \quad \text{power-law regime} \tag{20}$$

The difference between the mean square radius of gyration in the Guinier and power-law regimes is expected because large aggregates dominate scattering at small angles while small aggregates contribute more to the scattering pattern at large angles. Thus, using one definition for $\overline{R}_g^2$ at all scattering angles is not correct. Furthermore, at any angle, some of the aggregates are in the Guinier regime while others are in the power-law regime; thus, the crossover between small- and power-law behavior is more gradual for polydisperse aggregate populations than for individual aggregates.

The total scattering cross section of polydisperse aggregates is found from Eqs. (7) and (14) as follows:

$$\overline{C}_s^a = C_s^p \int_{N=1}^{\infty} N^2 g(kR_g, D_f) p(N) dN \tag{21}$$

Equation (21) must be numerically integrated, using Eq. (1) to relate R_g and N, after substituting for $g(kR_g, D_f)$ from Eqs. (8) and (9) and introducing the log-normal function for $p(N)$.

The absorption cross section of polydisperse aggregates can be evaluated easily from Eqs. (10) and (14), as follows:

Table 1 Structure and optical cross section properties of overfire soot[a]

Fuel	Acetylene	Propylene	Ethylene	Propane
Primary Particles:				
d_p (nm)	47	41	32	30
x_p (-)	0.287	0.250	0.195	0.183
C_{vv}^p (nm²/sr)	0.814	0.359	0.0811	0.0551
C_s^p (nm²)	6.82	3.01	0.679	0.462
C_e^p (nm²)	524	346	164	134
ρ_{sa}^p (-)	0.0132	0.0088	0.0042	0.0034
n_p (mm⁻³) × 10⁻⁶	6.2	6.4	2.6	2.5
Aggregates:				
$\overline{N}$ (-)	417	400	467	364
$\overline{C}_{vv}^a(90°)$ (nm²/sr)	3710	2370	1020	559
$\overline{C}_s^a$ (nm²) × 10⁻³	92.9	55.0	21.8	10.4
$\overline{C}_e^a$ (nm³) × 10⁻³	321	194	98.2	58.8
$\overline{\rho}_{sa}^a$ (-)	0.41	0.40	0.29	0.22
$\overline{\rho}_v^a$ (-)	0.041	0.033	0.028	0.022
n_a (mm⁻³) × 10⁻³	14	16	5.5	6.8

[a]For buoyant turbulent diffusion flames in still air at long residence times with optical properties at 514.5 nm: structure properties from Köylü and Faeth, (1992); soot refractive indices used in the computations from Dalzell and Sarofim (1969).

$$\overline{C}_a^a = \overline{N} C_a^p \tag{22}$$

Similar to a single aggregate, the extinction cross section can be written in terms of the ratio of scattering to absorption cross sections, $\overline{\rho}_{sa}^a = \overline{C}_s^a/\overline{C}_a^a$, to yield:

$$\overline{C}_e^a = \overline{N} C_a^p (1 + \overline{\rho}_{sa}^a) \tag{23}$$

where $\overline{\rho}_{sa}^a$ reduces to ρ_{sa}^a from Eq. (13) at the limit of large monodisperse aggregates.

Results and Discussion

Optical Cross Sections. The measured volumetric optical cross sections were converted to optical cross sections using the approximation that absorption is not affected by aggregation. Then the number of primary particles per unit volume, n_p, can be computed from

$$n_p = \overline{Q}_a^a / C_a^p \tag{24}$$

C_a^p was found from Eq. (2), given d_p from the structure measurements, and adopting the refractive indices of Dalzell and Sarofim (1969), i.e., $m = 1.57 + 0.56i$ at 514.5 and 632.8 nm and $1.65 + 0.75i$ at 1152 nm. The Dalzell and Sarofim (1969) refractive indices were used to be consistent with Köylü and Faeth (1992); however, they also are preferred based on the present scattering measurements, as discussed later. Then, given $\overline{N}$ from the soot structure measurements, the mean number of aggregates per unit volume, n_a, can be found from

$$n_a = n_p/\overline{N} \tag{25}$$

yielding the optical cross sections as follows:

$$\overline{C}_j^a(\theta) = \overline{Q}_j^a(\theta)/n_a; \quad j = pp, s, a \tag{26}$$

Soot Structure Parameters. Reference soot structure and optical cross section properties at 514.5 nm are summarized in Table 1 for the four fuels. The table also includes the primary particle properties and the values of $\overline{N}$ that were used to find the optical cross sections of aggregates, as well as the resulting values of n_p and n_a. At 514.5 nm, x_p is in the range 0.183–0.287, which marginally places the primary particles in the Rayleigh scattering regime (Kerker, 1969). The values of $\overline{\rho}_{sa}^a$ are roughly two orders of magnitude larger than ρ_{sa}^p, highlight-

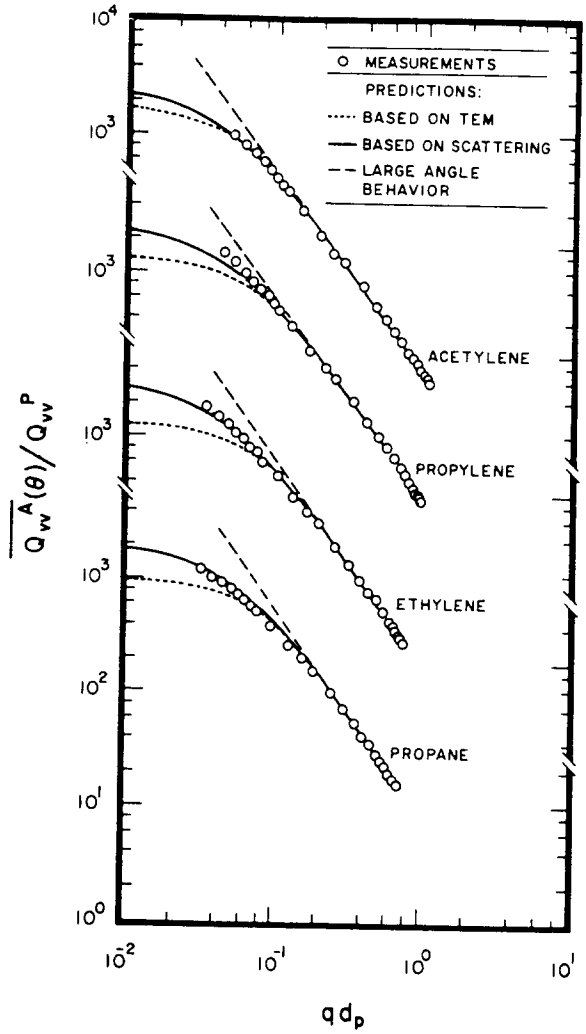

Fig. 2 Measured and predicted volumetric *vv* cross sections as a function of the modulus of the scattering vector

ing the much greater degree of scattering from aggregates than from individual primary particles. As discussed earlier, $\overline{\rho}_{sa}^{a}$ can be viewed as the error made when soot volume fractions are computed from laser extinction measurements using the small particle (Rayleigh) scattering limit. The results of Table 1 show that this practice causes errors of 22–41 percent for present conditions, increasing with increasing tendency of the fuel to soot. Nevertheless, it seems premature to correct earlier measurements of soot volume fractions at the same conditions (Sivathanu and Faeth, 1990) because current uncertainties of soot refractive indices can affect these results to a much larger extent, e.g., by roughly a factor of two (Dobbins and Megaridis, 1991).

Measured and predicted values of $\overline{Q}_{vv}^{a}(\theta)$ are plotted as a function of qd_p at 514.5 nm in Fig. 2 for the four fuels. Extrapolations of large-angle behavior also are shown on the plots for reference purposes. The substantial departure from Rayleigh scattering behavior (where $\overline{Q}_{vv}^{a}(\theta)$ would be independent of qd_p) is evident, with forward scattering roughly 100 times larger than large-angle scattering for all the fuels. The large size of the present soot aggregates, and the extended transition between the Guinier and power-law regimes due to polydisperse effects, prevented fully reaching the Guinier regime even though scattering angles as small as 5 deg were considered. However, the measurements provide an extended range within the power-law regime, e.g., roughly $qd_p > 0.1$.

The measurements in the power-law regime in Fig. 2 can be

Table 2 Soot aggregate fractal properties from thermophoretic sampling (*TS*) and light scattering (*LS*) measurements[a]

Fuel	D_f		k_f	
	TS	LS	TS[b]	LS[c]
Acetylene	1.79	1.85	9.2	7.0
Propylene	1.75	1.84	—	8.6
Ethylene	1.73	1.83	8.6	8.8
Propane	1.74	1.77	—	8.0

[a]For overfire soot from buoyant turbulent diffusion flames in still air at long residence times; light scattering measurements from the power-law regime at 514.5 nm.

[b]From Puri et al. (1993).

[c]Based on the soot refractive indices of Dalzell and Sarofim (1969).

interpreted to yield information about the fractal properties and refractive indices of the present overfire soot. At large angles, through Eqs. (19) and (26), the slope and magnitude of plots of $\overline{Q}_{vv}^{a}(\theta)$ as a function of qd_p yield D_f and k_f. These values are summarized Table 2 for the four fuels, along with values found from structure measurements using thermophoretic sampling and analysis with TEM. The values of D_f from the structure measurements of Köylü and Faeth (1992) and the present scattering measurements agree within experimental uncertainties and exhibit little variation with fuel type, yielding average values of 1.82 and 1.79 with standard deviations of 0.04 and 0.05, for the scattering measurements and over all the measurements. The fact that $D_f < 2$ implies fractal aggregate scattering behavior with scattering properties saturating when N is large, as suggested by Eq. (13), rather than Mie scattering for an equivalent sphere where ρ_{sa}^{a} continues to increase as N increases (Berry and Percival, 1986). Thus, aggregate sizes preclude Rayleigh scattering behavior while aggregate fractal dimensions preclude treating size effects by Mie scattering for an equivalent sphere. The variations of k_f with fuel type also are relatively small, yielding a mean value of 8.1 with a standard deviation of 0.8 over all the fuels (which is consistent with the estimated experimental uncertainty (95 percent confidence) of less than 23 percent for the k_f determinations). The present values of k_f are similar to the values found by Puri et al. (1993) of 9.2 and 8.6 for acetylene and ethylene flames from thermophoretic sampling measurements. Thus, both D_f and k_f appear to be relatively independent of fuel type for overfire soot aggregates.

Information about refractive indices can be obtained from the measurements in the power-law regime by finding $\overline{Q}_{vv}^{a}(\theta)/\overline{Q}_{a}^{a}$ from Eqs. (19), (22), and (26) and eliminating C_{vv}^{p} and C_{a}^{p} from this expression using Eq. (2). After rearranging, the following expression is obtained:

$$F(m)/E(m) = 4\pi(q\,d_p)^{D_f}\,\overline{Q}_{vv}^{a}(\theta)/(k_f x_p^3\,\overline{Q}_{a}^{a}), \quad \text{power-law regime} \quad (27)$$

All the quantities on the right-hand side of Eq. (27) are known from either the structure or power-law scattering measurements: d_p and x_p are summarized in Table 2, $D_f = 1.8$ and $k_f = 9.0$ are reasonable averages for present test conditions, based on the thermophoretic sampling results of Köylü and Faeth (1992) and Puri et al. (1993); while the values of $\overline{Q}_{a}^{a}$ are known from the present optical measurements. Then introducing $\overline{Q}_{vv}^{a}(\theta)$ at $\theta = 160$ deg, which is well within the power-law regime, yields $F(m)/E(m) = 0.74$ with a standard deviation of 0.09 over all the fuels. Available values of refractive indices at this wavelength include $m = 1.57 + 0.56i$ (Dalzell and Sarofim, 1969), $1.90 + 0.55i$ (Tien and Lee, 1982) and $1.63 + 0.48i$ (Chang and Charalampopoulos, 1990), yielding $F(m)/$

Table 3 Soot aggregate size distribution properties from thermophoretic sampling (*TS*) and light scattering (*LS*) measurements[a]

Fuel	N_g		σ_g		$\overline{N^2}/\overline{N}$	
	TS	LS	TS	LS	TS	LS
Acetylene	214	180	3.3	3.8	1330	1840
Propylene	227	162	3.0	3.9	1200	2860
Ethylene	290	189	2.7	3.9	1130	2390
Propane	224	162	2.9	3.6	930	2300

[a]For overfire soot from buoyant turbulent diffusion flames in still air at long residence times; light scattering measurements from near-Guinier regime at 514.5 nm. Light scattering measurements based on the soot refractive indices of Dalzell and Sarofim (1969); $\bar{N}$ for each fuel the same for both TS and LS measurements.

$E(m)$ = 0.84, 1.55, and 0.96, respectively. Thus, the measurements of Dalzell and Sarofim (1969) are most consistent with present soot aggregate scattering measurements when analyzed by the approximate theory developed in the previous section. These results also suggest that $F(m)/E(m)$ is relatively independent of fuel type for present conditions.

Two predictions based on the RDG polydisperse fractal aggregate theory are illustrated in Fig. 2, one entirely based on results from the structure (TEM) measurements, the other based on refitted aggregate size distributions (keeping $\bar{N}$ the same), which best match the scattering measurements. Both predictions use D_f = 1.8 and the individual k_f values deduced from the light scattering measurements for each fuel as summarized in Table 2. Since the predictions use the same $\bar{N}$, they yield identical results in the power-law regime through Eq. (19); they also are in good agreement with the measurements in this regime. However, predictions based on the structure measurements significantly underestimate scattering levels as the Guinier regime is approached. This is plausible due to the sampling limitations of the TEM measurements, where large aggregates that dominate forward scattering might not be found in sufficient quantities. In particular, the moment $\overline{N^2}$, which is crucial for scattering properties in the Guinier regime (see Eq. (17)), exhibited large uncertainties, 40–90 percent (see Table 3), suggesting potential sampling difficulties (Köylü and Faeth, 1992). Thus, the aggregate size distribution functions were refitted, keeping $\bar{N}$ constant as noted earlier, to achieve the reasonably good match of measured scattering properties in the transition regime illustrated in Fig. 2. The original (*TS*) and refitted (*LS*) aggregate size distribution parameters are summarized in Table 3 for all the fuels; changes of N_g and σ_g are within experimental uncertainties while the main difference between the thermophoretic sampling and scattering measurements is the higher order moment, $\overline{N^2}$, which easily is biased during TEM measurements due to sampling limitations, e.g., a small variation in the number of large aggregates in the sample will change this moment substantially. This suggests that the RDG polydisperse fractal aggregate theory provides a reasonable basis for treating overfire soot aggregates. However, additional study of the Guinier regime is needed to definitively evaluate the approach.

Angular Scattering Patterns. Predicted and measured angular scattering patterns at 514.5 nm are plotted in Figs. 3 and 4 for acetylene and ethylene as examples of strongly and weakly sooting fuels; results for propylene and propane were similar; see Köylü (1992). The predictions of $\overline{C}^a_{vv}(\theta)$ are based on the refitted soot structure properties from the light scattering measurements, and are in excellent agreement with the measurements as discussed in connection with Fig. 2. These results clearly show very strong scattering at small values of θ. The

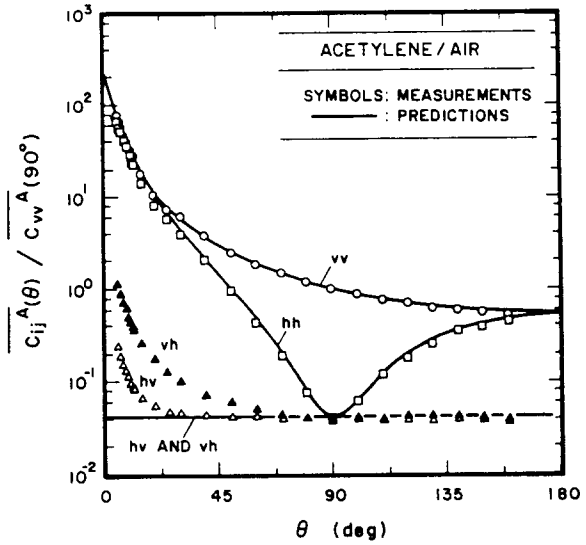

Fig. 3 Measured and predicted angular scattering patterns of overfire soot aggregates in turbulent acetylene/air diffusion flames

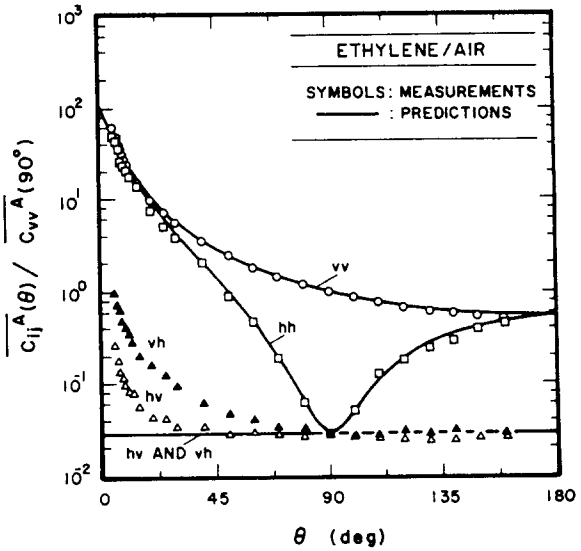

Fig. 4 Measured and predicted angular scattering patterns of overfire soot aggregates in turbulent ethylene/air diffusion flames

formulations for *hh*, *vh*, and *hv* scattering cross sections were modified slightly to account for observed depolarization effects. This was done by introducing depolarization ratios for soot aggregates, $\bar{\rho}^a_v$, analogous to Rayleigh scattering theory (Rudder and Bach, 1968), as follows:

$$\overline{C}^a_{hh}(\theta) = \overline{C}^a_{vv}(\theta)[(1-\bar{\rho}^a_v)\cos^2\theta + \bar{\rho}^a_v] \quad (28)$$

$$\overline{C}^a_{hv} = \overline{C}^a_{vh} = \overline{C}^a_{vv}(90 \text{ deg})\bar{\rho}^a_v \quad (29)$$

The measured values of $\bar{\rho}^a_v$ are summarized in Table 1; they increase with increasing propensity of the fuel to soot and generally are an order of magnitude larger than values found for Rayleigh scattering from molecules (Rudder and Bach, 1968). The resulting predictions of $\overline{C}^a_{hh}(\theta)$ are excellent, similar to $\overline{C}^a_{vv}(\theta)$. The predicted and measured scattering cross sections for the *vh* and *hv* components also are in good agreement with Rayleigh scattering ideas, except near the forward-scattering direction where the measured values increase and the *vh* and *hv* components no longer are equal. This behavior may be caused by experimental difficulties because uncertainties increase for both the *vh* and *hv* scattering components in the forward scattering direction due to effects of polarization vec-

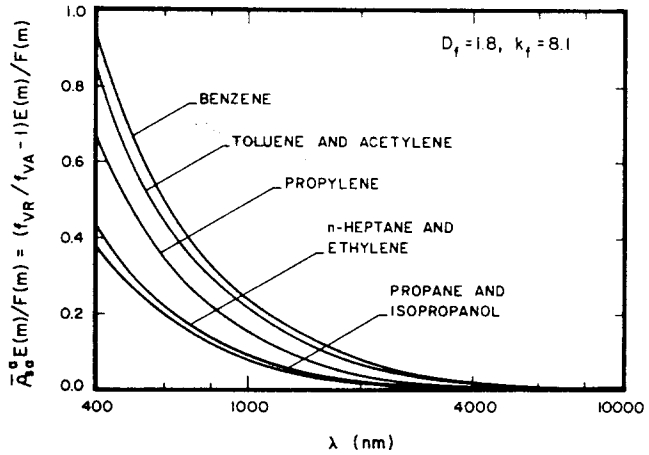

Fig. 5 Mean ratios of scattering to absorption cross sections as a function of wavelength for overfire soot aggregates in turbulent diffusion flames based on the predictions of the RDG polydisperse fractal aggregate theory

Table 4 Measured and predicted extinction cross sections, $\bar{C}^a_s$ (nm²) × 10^{-3}, for overfire soot aggregates[a]

Fuel	Acetylene	Propylene	Ethylene	Propane
514.5 nm:				
Measured	321	194	98.2	58.8
Predicted[b]	321	194	98.2	59.3
632.8 nm:				
Measured	290	172	73.1	43.7
Predicted[b]	248	143	74.7	46.5
1152 nm:				
Measured	176	86.8	45.5	26.9
Predicted[b]	144	84.4	45.3	28.4

[a]For buoyant turbulent diffusion flames in still air at long residence times.
[b]Based on the laser scattering properties of soot aggregates fitted at 514.5 nm and the soot refractive indices of Dalzell and Sarofim (1969).

tor misalignment when scattering is strong. In particular, experimental problems are suggested in this region because there is no fundamental reason for the *vh* and *hv* scattering components to differ for randomly oriented aggregates of small primary particles. However, the behavior also may reflect limitations of the RDG theory due to effects of multiple scattering in the forward direction. Thus, additional theoretical consideration of the depolarization ratios of soot aggregates would be interesting to help assess both the experimental and theoretical limitations of present methods. As a practical matter, however, the *vh* and *hv* components are small in comparison to *vv* and *hh* scattering and can be neglected for typical scattering calculations.

Extinction at Various Wavelengths. Extinction cross sections at 514.5, 632.8, and 1152 nm were measured in order to evaluate the capabilities of the RDG polydisperse fractal aggregate theory to estimate optical cross sections at various wavelengths. The results of these measurements and predictions are summarized in Table 4. The predictions are based on $D_f = 1.8$, $k_f = 8.1$ as reasonable averages of present estimates of fractal properties from Table 2, the aggregate size distribution properties from the scattering data summarized in Table 3, and the refractive indices of Dalzell and Sarofim (1969) listed earlier. Measured and predicted extinction cross sections at 514.5 nm are in close agreement, but this is not very significant because soot structure and optical properties were matched at this condition. Nevertheless, predicted extinction cross sections are within 18 percent of the measurements at both 632.8 and 1152 nm, with the largest errors exhibited for heavily sooting fuels like acetylene and propylene; this is good agreement in view of the uncertainties of soot refractive indices and the approximate nature of the scattering theory.

The present RDG polydisperse fractal aggregate theory was used to estimate the scattering contribution to extinction at other wavelengths since the predictions were reasonably good at the wavelengths where measurements were made. The predicted ratios of scattering to absorption cross sections are illustrated as a function of wavelength in Fig. 5. Results are shown for both the gaseous and liquid fuels studied by Köylü and Faeth (1992), using $D_f = 1.8$ and $k_f = 8.1$ as before. The soot aggregate size distribution parameters (N_g and σ_g) for these calculations were drawn from the thermophoretic sampling measurements of Köylü and Faeth (1992), even though present scattering measurements for gaseous fuels suggested the need for adjusting these parameters somewhat, see Table 3. This is justified because total scattering predictions using the thermophoretic sampling measurements agreed with present measurements within 15 percent, because the changes of the size distribution parameters only affected results at very small angles. The predictions are presented as $\bar{\rho}^a_{sa}\,E(m)/F(m)$ to avoid complications due to the considerable uncertainties of soot refractive indices discussed earlier. The plot of Fig. 5 updates results reported by Köylü and Faeth (1992), based on the RDG polydisperse fractal aggregate theory of Dobbins and Megaridis (1991), which is mainly designed to treat the Guinier regime as discussed earlier; there are quantitative differences between the two sets of results but the general trends are similar.

The plots of $\bar{\rho}^a_{sa}$ in Fig. 5 indicate departure of aggregate scattering properties from the small particle (Rayleigh) scattering limit. The results show that this departure is greatest for strongly sooting fuels like toluene, benzene, and acetylene in the visible portion of the spectrum. Noting that $F(m)/E(m)$ is of order unity, soot volume fractions would be overestimated by 20–50 percent for laser extinction measurements at 632.8 nm, analyzed using the Rayleigh scattering approximation. The value of $\bar{\rho}^a_{sa}$, however, decreases with increasing wavelength and becomes relatively small for wavelengths greater than 2000 nm. Thus, the effect of aggregate scattering appears to be relatively small for estimates of soot radiation properties in the infrared, when compared with other uncertainties of such calculations, even for the present rather large overfire soot aggregates.

Discussion. The reasonably good overall comparison between predictions using the RDG polydisperse fractal aggregate theory and the present measurements is promising. However, the evaluation was limited with respect to the general effectiveness of the RDG scattering approximation for treating soot optical properties. First of all, the large size of the present aggregates implied that the bulk of the measurements were in the power-law regime. In this regime, the computations of Nelson (1989) suggest that effects of multiple scattering are relatively small, and that the RDG approximation of Eq. (5) is satisfactory even for large aggregates. Thus, while it is encouraging that predictions based solely on structure measurements were satisfactory in this regime, this does not constitute a definitive evaluation of the RDG approximation for soot aggregates.

Effects of multiple scattering are most significant for forward scattering in the Guinier regime, which would provide a strong test of the RDG scattering approximation. Unfortunately, two difficulties were encountered during the present evaluation of predictions in this regime. First of all, the large size of the present aggregates precluded fully reaching the Guinier regime for experimentally accessible scattering angles so that the full effect of potential multiple scattering was not observed. Secondly, it was necessary to refit the aggregate size distribution function, to increase the higher moment $\overline{N^2}$, in

order to match the scattering data. While such refitting is plausible due to the sampling limitations of the structure measurements, as discussed earlier, the refitting also could mask fundamental deficiencies of the RDG scattering approximation. Thus, while it is encouraging that the RDG polydisperse fractal aggregate approach seems capable of correlating the present measurements of soot optical properties, and scattering measurements eventually may prove to be the best way to find the higher moments of the soot aggregate size distributions, additional evaluation of the RDG approximation is needed. This will require measurements of both structure and optical properties for soot populations having smaller aggregates and thus a more extensive Guinier regime.

Conclusions

The optical properties of overfire soot were measured for buoyant turbulent diffusion flames burning in still air. The fuels considered included acetylene, propylene, ethylene, and propane. Measurements were limited to the long residence time regime where soot structure was known from earlier thermophoretic sampling measurements (Köylü and Faeth, 1992), and is independent of position and residence time in the overfire region. The combined soot structure and optical property measurements were used to evaluate an approximate RDG polydisperse fractal aggregate theory of soot optical properties. The main conclusions of the study are as follows:

1 The optical properties of the present soot at 514.5 nm departed significantly from Rayleigh scattering behavior: Forward scattering was roughly 100 times larger than large-angle scattering, total scattering was 22–41 percent of absorption, and depolarization ratios were roughly an order of magnitude larger than values typical of Rayleigh scattering from molecules. This causes soot volume fractions to be overestimated up to 70 percent for heavily sooting fuels when laser extinction measurements in the visible are interpreted using the Raleigh scattering approximation; see Fig. 5.

2 The present scattering measurements in the power-law regime yield aggregate fractal properties that are relatively independent of fuel type, as follows: fractal dimension, D_f = 1.82 with a standard deviation of 0.04; and fractal prefactor, k_f = 8.1 with a standard deviation of 0.09. These values agree within experimental uncertainties with earlier structure measurements for overfire soot obtained by thermophoretic sampling (Köylü and Faeth, 1992; Puri et al., 1993), and appear to be relatively robust properties of overfire soot aggregates.

3 Present scattering measurements in the power-law regime at 514.5 nm yielded the soot refractive index ratio, $F(m)/E(m)$ = 0.74 with a standard deviation of 0.09, over all the fuels. The refractive index measurements of Dalzell and Sarofim (1969) yield $F(m)/E(m)$ = 0.84, which is in good agreement with present observations, while newer values from Tien and Lee (1982) and Chang and Charalampopoulos (1990) are somewhat higher, 1.55 and 0.96, respectively. The continued uncertainties of soot refractive indices are a substantial limitation to reliable nonintrusive laser-based measurements of soot properties and should be resolved.

4 The RDG polydisperse fractal aggregate theory provided reasonably good predictions of present soot optical property measurements. This was accomplished with predictions based solely on soot structure measurements in the power-law regime, and after refitting the aggregate size distribution in the Guinier regime in order to adjust $\overline{N^2}$ since it could not be determined very accurately from the structure measurements. While this is promising, present measurements only approached the Guinier regime where potential deficiencies of the RDG scattering approximation should be most apparent. Thus, additional work at conditions that extend farther into the Guinier regime is needed in order to establish reliably the effectiveness of the RDG approximation for soot optical properties.

Acknowledgments

This research was supported by the Building and Fire Research Laboratory of the National Institute of Standards and Technology, Grant No. 60NANB1D1175, with H. R. Baum serving as Scientific Officer.

References

Berry, M. V., and Percival, I. C., 1986, "Optics of Fractal Clusters Such as Smoke," *Optica Acta*, Vol. 33, pp. 577–591.

Bohren, C. F., and Huffman, D. R., 1983, *Absorption and Scattering of Light by Small Particles*, Wiley, New York, pp. 477–482.

Chang, H., and Charalampopoulos, T. T., 1990, "Determination of the Wavelength Dependence of Refractive Indices of Flame Soot," *Proc. R. Soc. London A*, Vol. 430, pp. 577–591.

Chen, H. Y., Iskander, M. F., and Penner, J. E., 1990, "Light Scattering and Absorption by Fractal Agglomerates and Coagulations of Smoke Aerosols," *J. Modern Optics*, Vol. 2, pp. 171–181.

Dalzell, W. H., and Sarofim, A. F., 1969, "Optical Constants of Soot and Their Application to Heat Flux Calculations," ASME JOURNAL OF HEAT TRANSFER, Vol. 91, pp. 100–104.

Dalzell, W. H., Williams, G. C., and Hottel, H. C., 1970, "A Light Scattering Method for Soot Concentration Measurements," *Combust. Flame*, Vol. 14, pp. 161–170.

Dobbins, R. A., and Megaridis, C. M., 1991, "Absorption and Scattering of Light by Polydisperse Aggregates," *Appl. Optics*, Vol. 30, pp. 4747–4754.

Erickson, W. D., Williams, G. C., and Hottel, H. C., 1964, "Light Scattering Measurements on Soot in a Benzene-Air Flame," *Combust. Flame*, Vol. 8, pp. 127–132.

Guinier, A., and Fournet, G., 1955, *Small-Angle Scattering of X-Rays*, Wiley, New York.

Jullien, R., and Botet, R., 1987, *Aggregation and Fractal Aggregates*, World Scientific Publishing Co., Singapore, pp. 46–50.

Kerker, M., 1969, *The Scattering of Light*, Academic Press, New York, pp. 414–486.

Köylü, Ü. Ö., 1992, "Emission, Structure and Optical Properties of Overfire Soot From Buoyant Turbulent Diffusion Flames," Ph.D. Thesis, The University of Michigan, Ann Arbor, MI.

Köylü, Ü. Ö., and Faeth, G. M., 1992, "Structure of Overfire Soot in Buoyant Turbulent Diffusion Flames at Long Residence Times," *Combust. Flame*, Vol. 89, pp. 140–156.

Köylü, Ü. Ö., and Faeth, G. M., 1993, "Radiation Properties of Flame-Generated Soot," ASME JOURNAL OF HEAT TRANSFER, Vol. 115, pp. 409–417.

Ku, J. C., and Shim, K.-H., 1992, "Optical Diagnostics and Radiative Properties of Simulated Soot Agglomerates," ASME JOURNAL OF HEAT TRANSFER, Vol. 113, pp. 953–958.

Magnussen, B. F., 1974, "An Investigation Into the Behavior of Soot in a Turbulent Free Jet C_2H_2-Flame," *Fifteenth Symposium (International) on Combustion*, The Combustion Institute, Pittsburgh, PA, pp. 1415–1425.

Martin, J. E., and Hurd, A. J., 1987, "Scattering From Fractals," *J. Appl. Cryst.*, Vol. 20, pp. 61–78.

Nelson, J., 1989, "Test of a Mean Field Theory for the Optics of Fractal Clusters," *J. Modern Optics*, Vol. 36, pp. 1031–1057.

Puri, R., Richardson, T. F., Santoro, R. J., and Dobbins, R. A., 1993, "Aerosol Dynamic Processes of Soot Aggregates in a Laminar Ethene Diffusion Flame," *Combust. Flame*, Vol. 92, pp. 320–333.

Rudder, R. R., and Bach, D. R., 1968, "Rayleigh Scattering of Ruby-Laser Light by Neutral Gases," *J. Opt. Soc. Amer.* Vol. 58, pp. 1260–1266.

Sivathanu, Y. R., and Faeth, G. M., 1990, "Soot Volume Fractions in the Overfire Region of Turbulent Diffusion Flames," *Combust. Flame*, Vol. 81, pp. 133–149.

Tien, C. L., and Lee, S. C., 1982, "Flame Radiation," *Prog. Energy Combust. Sci.*, Vol. 8, pp. 41–59.

van de Hulst, H. C., 1957, *Light Scattering by Small Particles*, Dover Publications, New York.

Wersborg, B. L., Howard, J. B., and Williams, G. C., 1972, "Physical Mechanisms in Carbon Formation in Flames," *Fourteenth Symposium (International) on Combustion*, The Combustion Institute, Pittsburgh, pp. 929–940.